PROCEEDINGS OF SCIENCE

Entangled neutral kaons as a tool for precision tests of CPT symmetry and Quantum Mechanics from KLOE-2

Wojciech Wiślicki[a,*] **on behalf of the KLOE-2 Collaboration**

[a] *National Centre for Nuclear Research,*
7 Pasteura, 02-093 Warszawa, Poland

E-mail: wojciech.wislicki@ncbj.gov.pl

The quantum interference between entangled neutral kaons from decays $\phi(1020) \to K_L K_S \to (\pi^+\pi^-)(\pi^+\pi^-)$ was measured in the KLOE detector at the DAΦNE electron-positron collider. Shape of the interference pattern exhibits very high sensitivity to possible decoherence of kaons and violation of the fundamental $\mathcal{CPT}$ symmetry. This pattern was analysed in the Δt variable, being the difference of times of kaon decays, using 1.7×10^9 decays of $\phi^0 \to K_L K_S$ [1]. Fits of models of decoherence and $\mathcal{CPT}$ violation significantly improves accuracy of their parameters with respect to earlier measurements [2].

8th Symposium on Prospects in the Physics of Discrete Symmetries (DISCRETE 2022)
7-11 November, 2022
Baden-Baden, Germany

*Speaker

PoS(DISCRETE2022)066

1. Introduction

Testing quantum entanglement by using pairs of neutral kaons was first proposed in early 1960's when the authors of refs [3–5] recognized how to use such pairs in the C-odd state (C stands for charge conjugation) for research on the Einstein-Podolsky-Rosen paradox. Coherent pairs of neutral kaons, in the basis of their mass eigenstates K_L and K_S, are produced in ϕ^0 decays in the $J^{PC} = 1^{--}$ state

$$|\psi\rangle \quad = \quad \frac{N}{\sqrt{2}}(|K_S\rangle|K_L\rangle - |K_L\rangle|K_S\rangle), \tag{1}$$

where N depends on the CP-violation parameters. The decay intensity of $|\psi\rangle$ to the final state $|f\rangle = |\pi^+\pi^-\,\pi^+\pi^-\rangle$ as a function of kaons' proper decay times $t_{1,2}$ is equal to

$$|\langle f|\psi(t_1,t_2)\rangle|^2 \quad \sim \quad e^{-\Gamma_L t_1-\Gamma_S t_2} + e^{-\Gamma_S t_1-\Gamma_L t_2} - 2e^{-(\Gamma_L+\Gamma_S)(t_1+t_2)/2}\cos(\Delta m\Delta t), \tag{2}$$

where $\Gamma_{L,S}$ are decay widths and $\Delta m = m_L - m_S$ is the mass difference, where indexes $_{L,S}$ refer to $K_{L,S}$, and $\Delta t = |t_2 - t_1|$. Explicit dependence on decay amplitudes is factored out in eq. (2).

Possible loss of entanglement of the state (1) may lead to a factorizable state of the kaon pair. Without further assumptions on its physical mechanism such transition was first considered in ref. [6] and is called Furry hypothesis. Its simplest parametrization was proposed in ref. [7] which in the $\{K_L, K_S\}$ basis reads

$$|\langle f|\psi(t_1,t_2,\zeta_{LS})\rangle|^2 \sim \\ e^{-\Gamma_L t_1-\Gamma_S t_2} + e^{-\Gamma_S t_1-\Gamma_L t_2} - 2(1-\zeta_{LS})e^{-(\Gamma_L+\Gamma_S)(t_1+t_2)/2}\cos(\Delta m\Delta t). \tag{3}$$

The real parameter $0 \le \zeta_{LS} \le 1$ quantifies the degree of coherence: $\zeta_{LS} = 0$ corresponds to the coherent state and $\zeta_{LS} = 1$ to the factorized state, i.e. completly destroyed coherence. Expressions similar to eq. (3) can be found in the $\{K^0, \bar{K}^0\}$ basis using parameter $\zeta_{0\bar{0}}$, where dependence on the amplitudes cannot be factored out. Another model incorporates a time-dependent $\zeta_{LS}(t_1,t_2) = \exp[-\lambda\min(t_1,t_2)]$ [1, 7]. In this case a simple relation between ζ_{LS} and λ can be found after integration over $t_1 + t_2$

$$\zeta_{LS} \quad = \quad \frac{\lambda}{\Gamma_L+\Gamma_S+\lambda} \simeq \frac{\lambda}{\Gamma_S}. \tag{4}$$

Another approach, called the γ-model henceforth, incorporates the mechanism of environmental decoherence to description of the decay spectrum. Theoretical framework is based on modification of the classical Liouville - von Neumann dynamics for dissipative systems in terms of density matrix, as presenterd by authors of refs [8, 9] and adopted for the neutral kaon pair in refs [10, 11]

$$\frac{\partial\rho}{\partial t} \quad = \quad i[\rho, H] + L(\rho;\alpha,\beta,\gamma), \tag{5}$$

where H stands for the effictive Hamiltonian of the kaon pairs and L for a dissipative term, parametrized with real parameters α, β, γ that may induce decoherence and violate the $\mathcal{T}$ and $\mathcal{CPT}$ symmetry ($\mathcal{T}$ is time reversal and $\mathcal{P}$ space inversion) due to dissipative arrow of time. Posing

requirement of the completly positive evolution [12] implies $\alpha = \gamma$ and $\beta = 0$ and thus simplifies the model to one parameter.

In a trial to set a limit on the explicit $\mathcal{CPT}$ violation, a proposal of ref. [13] assumes that the initial state (1) contains also admixture of states with a wrong $\mathcal{CPT}$ and reads

$$|\psi\rangle \quad \sim \quad |K_S\rangle|K_L\rangle - |K_L\rangle|K_S\rangle + \omega(|K_S\rangle|K_S\rangle - |K_L\rangle|K_L\rangle), \tag{6}$$

where ω is a complex parameter quantifying it. This approach is further called the ω-model. Both the γ- and ω-models constitute frameworks capable to connect experimental data to theoretical proposals of physics extending beyond the Standard Model of interactions, e.g. to quantum-gravitational concepts of space-time backgrounds at the Planck scale (cf. ref. [14] and references therein).

2. The KLOE detector at DAΦNE

The data were collected with the KLOE detector at the DAΦNE e^+e^- collider [15], that operates at a center-of-mass energy corresponding to the mass of the ϕ^0 meson, i.e. 1019 MeV. Positron and electron beams of equal energy collide at an angle of $(\pi - 0.025)$ rad, producing ϕ^0 mesons with a small momentum in the horizontal plane, $p_\phi \simeq 13$ MeV, and decaying 34% of the time into nearly collinear $K_L\,K_S$ pairs.

The data sample analyzed in the present work corresponds to an integrated luminosity of 1.7 fb^{-1} corresponding to 1.7×10^9 $\phi^0 \to K_L K_S$ decays.

The detector consists of a large cylindrical drift chamber surrounded by a lead/scintillating-fiber sampling calorimeter (EMC). A superconducting coil surrounding the calorimeter provides a 0.52 T magnetic field. Details of the KLOE spectrometer are given in refs [16, 17].

The momentum resolution of the spectrometer is equal to $\sigma(p_\perp)/p_\perp = 0.4\%$, and the $K_S \to \pi^+\pi^-$ invariant mass is reconstructed with a resolution of 1 MeV. The calorimeter is divided into a barrel and two endcaps, covering 98% of the solid angle. The energy and time resolutions are $\sigma_E/E = 5.7\%/\sqrt{E(\mathrm{GeV})}$ and $\sigma_t = 54$ ps$/\sqrt{E(\mathrm{GeV})} \oplus 100$ ps, respectively.

The trigger [18] uses a two level scheme. The first level trigger is a fast trigger with a minimal delay which starts the acquisition of the EMC front-end-electronics. The second level trigger is based on the energy deposits in the EMC (at least 50 MeV in the barrel and 150 MeV in the end-caps) or on the hit multiplicity information from the DC. The trigger conditions are chosen to minimise the machine background, and recognise Bhabha scattering or cosmic-ray events. Both the calorimeter and drift chamber triggers are used for recording interesting events.

The response of the detector to the decays of interest and the various backgrounds are studied by using the KLOE Monte Carlo (MC) simulation program [19]. Changes in the machine operation and background conditions are taken into account. The MC samples used in the present analysis amount to an equivalent integrated luminosity of 17 fb^{-1} for the signal, and to 3.4 fb^{-1} for all main ϕ^0 decay channels.

3. Event selection and background

Selection of events is based on reconstructed two vertices of decays into $\pi^+\pi^-$ pairs. For each vertex, preselection criteria on the invariant mass of the pion pair and its total energy were applied,

and then an overall kinematic fit was performed, including the ϕ^0 and kaon vertices. For each $\pi^+\pi^-$ vertes an opening angle $\theta_{\pi\pi}$ was required $\cos\theta_{\pi\pi} > -0.975$. The resolution on Δt amounts to $0.7\tau_S$.

There are two main background sources after the selection for the signal described above: the non-resonant production of four pions, $e^+e^- \to \pi^+\pi^-\pi^+\pi^-$, and kaon regeneration on the beam pipe. The remaining background due to semileptonic K_L decays can be considered negligible, being uniformly distributed in Δt, and amounting in total from MC to less than 0.2% in the range $0 \le \Delta t < 12\,\tau_S$. The background from $e^+e^- \to \pi^+\pi^-\pi^+\pi^-$ is evaluated by studying the two-dimensional invariant mass distribution of the reconstructed kaon decay vertices in bins of Δt. In the distribution corresponding to $0 \le \Delta t < 1\,\tau_S$, shown in Fig. 1, the signal peak at the center and the background contribution distributed along the second diagonal (due to a correlation introduced by the selection and by kinematical constraints) can be identified. An unbinned maximum likelihood fit is performed in order to evaluate the number of background events.

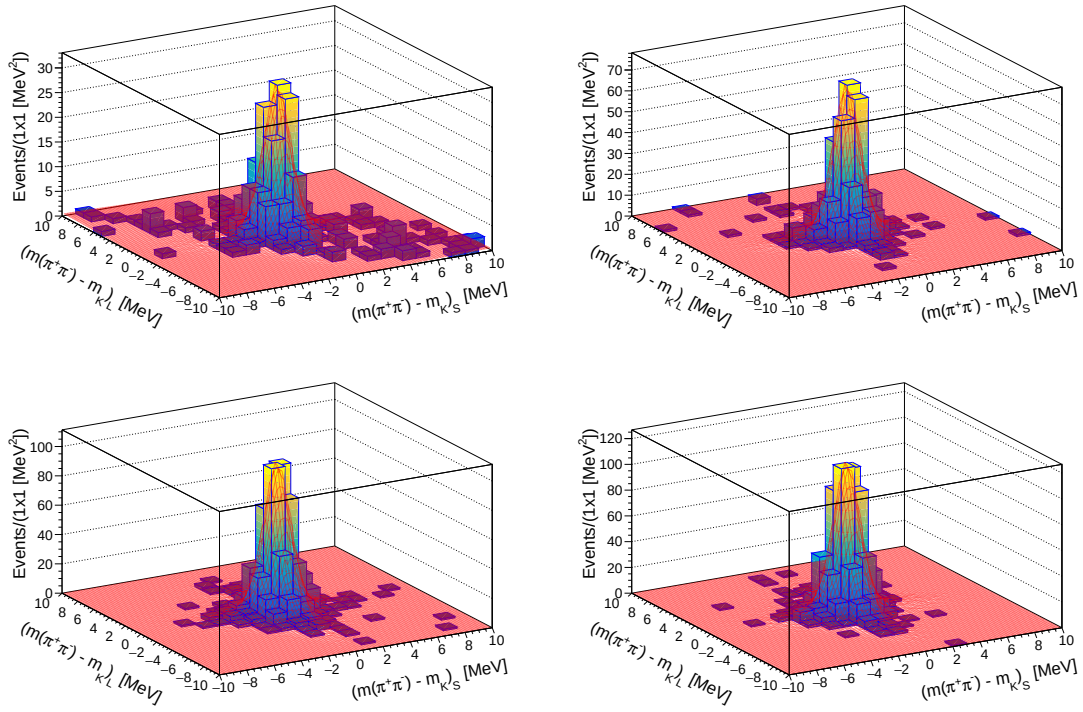

Figure 1: Invariant mass distribution of K_L vs. K_S vertices for four Δt bins: $0 \le \Delta t < 1\tau_S$ (top left), $1 \le \Delta t < 2\tau_S$ (top right), $2 \le \Delta t < 3\tau_S$ (bottom left), and $3 \le \Delta t < 4\tau_S$ (bottom right). The histograms of data have superimposed the result of the unbinned fit (red)

4. Efficiency and systematic uncertainties

Total efficiency of event selection was determined as a function of Δt using MC simulation. It consists of three factors: efficiency of the trigger, reconstruction and selection cuts. Fig. 2 (left) shows the efficiency as determined: after preselection cuts, after kinamatic fit and after cut

on the opening angle of pions from kaon vertices $\theta_{\pi\pi}$. Drop of efficiency at small Δt is due to longer extrapolation length for both tracks originating in the interaction point that enhances the probability to fail the reconstruction and a possible swap of tracks associated to two different kaon decay vertices, when the two vertices are close in time.

The trigger and reconstruction efficiencies provided by MC were checked with data, using an independent control sample of $K_S K_L \to \pi^+\pi^-\ \pi e\nu$ events, selected to have high purity and to have an overlap with the momentum distribution of the signal. The applied selection criteria ensure the statistical independence of the control sample from the signal and a purity of 95%, with the residual background dominated by the $K_S K_L \to \pi^+\pi^-\ \pi e\nu$ decay. The efficiency correction was evaluated as the ratio between data and MC Δt distributions of $K_S K_L \to \pi^+\pi^-\ \pi e\nu$ events. A fit with a constant indicates a quite small average correction, as shown in Fig. 3 (right).

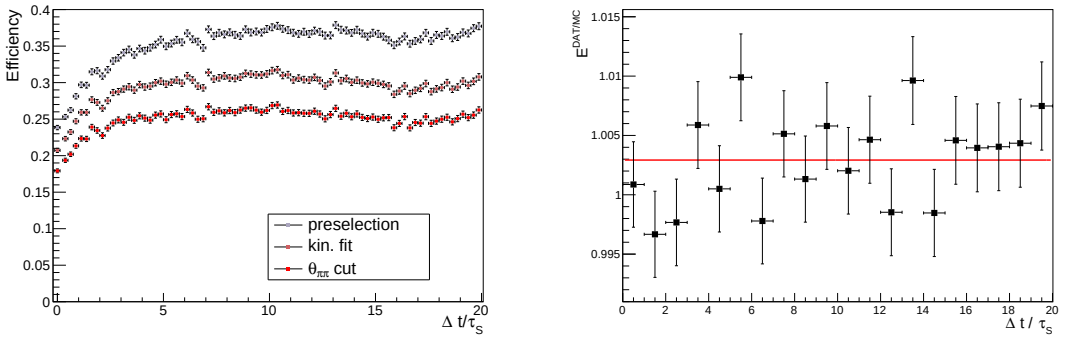

Figure 2: Efficiencies as functions of Δt. Left: Efficiency evaluated from the Monte Carlo, after the preselection criteria applied (grey), the kinematic fit (brown), and the cut on the $\theta_{\pi\pi}$ angle (red). The vertical error bars indicate the statistical uncertainty of the Monte Carlo sample. Right: Data/MC efficiency correction. The superimposed line is the result of a fit with a constant.

5. Results and Conclusions

	Furry hypothesis		γ-model
	ζ_{SL}	ζ_{00}	γ (GeV)
value	$(0.1 \pm 1.6 \pm 0.7) \times 10^{-2}$	$(-0.05 \pm 0.80 \pm 0.37) \times 10^{-6}$	$0.13 \pm 0.94 \pm 0.42) \times 10^{-21}$
χ^2/ndf	11.2/10		11.2/10

	ω-model			
	$\Re(\omega)$ (10^{-4})	$\Im(\omega)$ (10^{-4})	ϕ_ω (rad)	$\lvert\omega\rvert$ (10^{-4})
value	$-2.3^{+1.9}_{-1.5} \pm 0.7$	$-4, 1^{+2.8}_{-2.6} \pm 4.9$	$-2.1 \pm 0.2 \pm 0.1$	$4.7 \pm 2.9 \pm 1.0$
χ^2/ndf	9.2/9			

Table 1: Results of fits of three models of decoherence (3), (5) and (6) to experimental data. In each case the first error is statistical and the second is systematic.

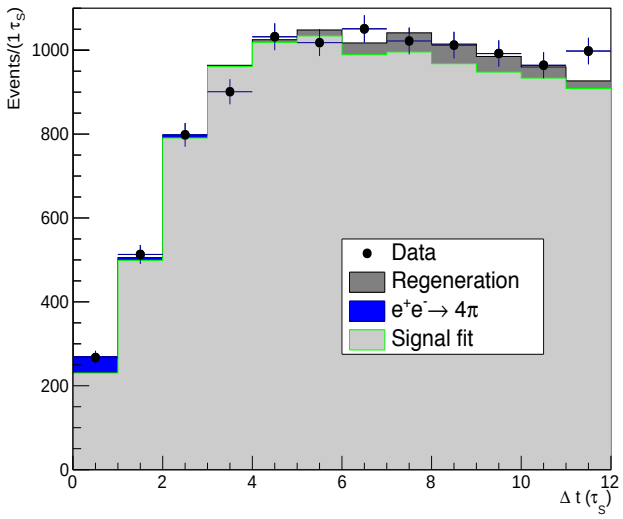

Figure 3: Data and fit distribution for the ζ_{SL} decoherence model with background contributions displayed.

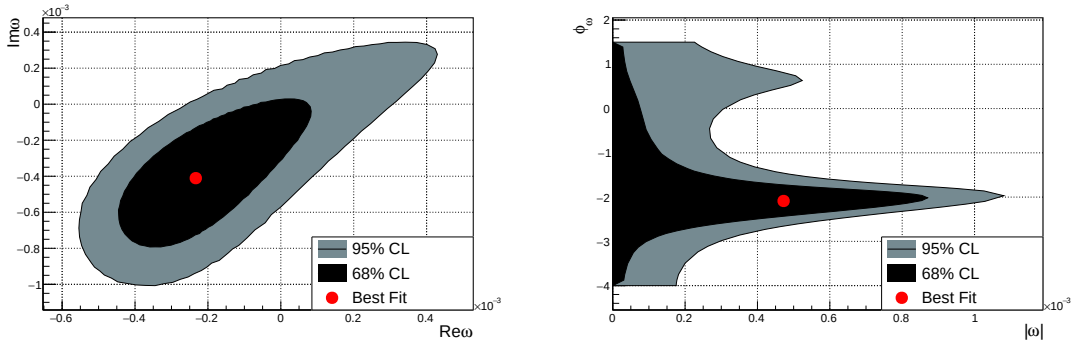

Figure 4: Results of a fit of the ω-model to experimental data. Left: Contour plot of the $\Im\omega$ vs. $\Re\omega$ for 68% and 95% confidence levels. Right: Contour plot of the ϕ_ω vs. $|\omega|$ for 68% and 95% confidence levels.

Results of the fits of three models of decoherence, (3), (5) and (6), are summarized in Tab. 1. Experimental distribution of Δt, together with the fit of ζ_{LS} in green, is shown in Fig. 3. Dominant sources of background, coming from the regeneration of K_S for large Δt and from nonresonant pion production $e^+e^- \to \pi^+\pi^-\pi^+\pi^-$ for small Δt, are also presented. Decoherence parameters ζ_{LS} and $\zeta_{0\bar{0}}$ are consistent with the null hypothesis of coherent evolution within one standard deviation. Higher precision on $\zeta_{0\bar{0}}$ is due to the fact that for small Δt the state $K^0\bar{K}^0$ has contribution from K_SK_S that is not $\mathcal{CP}$-suppressed and thus more likely decays into four pions, compared to K_LK_S. The λ parameter [7] of eq. (4) can be calculated from ζ_{LS} and it amounts to

$$\lambda \quad = \quad (0.1 \pm 1.2_{stat} \pm 0.5_{syst.}) \times 10^{-16}\ \text{GeV}. \tag{7}$$

Results of the fit of decoherence parameters can be also presented in terms of the upper limits at

the 90% confidence level as

$$\begin{aligned} \zeta_{LS} &< 0.030 \\ \zeta_{0\bar{0}} &< 1.4 \times 10^{-6} \\ \lambda &< 2.2 \times 10^{-16}\ \text{GeV} \\ \gamma &< 1.8 \times 10^{-21}\ \text{GeV}. \end{aligned} \tag{8}$$

Since the ω parameter in model (6) is complex, fits of the ω-model can be performed either in the Cartesian or in polar representations. Besides Tab. 1, results of those fits are presented in Fig. 4 where also the confidence contours corresponding to the one- and two standard deviations are given. It is seen that all parametrs $\Re\omega$, $\Im\omega$, $|\omega|$ and ϕ_ω are consistent with zero within one standard deviation. Due to nonlinear dependence of the state (6) on ϕ_ω in the polar representation, the shape of contours is not elliptic and consistency of ϕ_ω with zero within 1-σ contour is seen in Fig. 4 and not from values of its error in the minmum of χ^2.

These results [1] represent an improvement with respect to the previuos KLOE [2] and earlier CPLEAR measurements [20, 21]. All results are consistent with no decoherence and no $\mathcal{CPT}$ symmetry violation. The values of parameters γ and ω obtained from the fit are close to the Planck scale where the quantum-gravitational space-time background effects may play role (cf. contributions to ref. [14]). The Planck-scale effects on γ and ω should be of the order of $m_K^2/m_P \sim 10^{-20}$ and $\sqrt{m_K^2/(m_P(\Gamma_S - \Gamma_L))} \sim 10^{-3}$, respectively, where $m_P = 1.2 \times 10^{19}$ GeV is the Planck mass.

6. Acknowledgements

This work was supported in part by the Polish National Science Centre through the Grant No. 2017/26/M/ST2/00697.

References

[1] KLOE-2 Collaboration, D. Babusci et al., *Precision tests of quantum mechanics and CPT symmetry with entangled neutral kaons at KLOE*, *JHEP* **04** (2022) 059, [hep-x/2111.04328].

[2] KLOE Collaboration, F. Ambrosino et al., *First observation of quantum interference in the process $\phi \to K_S K_L \to \pi^+\pi^-\pi^+\pi^-$: A Test of quantum mechanics and CPT symmetry*, *Phys. Lett.* **B 642** (2006) 315, [hep-ex/0607027].

[3] T.D. Lee and C.Y. Yang, *Reported by T.D. Lee at the Argonne National Laboratory*, unpublished (1960).

[4] T.B. Day, *Demonstration of Quantum Mechanics in the Large*, *Phys. Rev.* **121** (1961) 1204.

[5] D.R. Inglis, *Completeness of Quantum Mechanics and Charge-Conjugation correlations of Theta particles*, *Rev. Mod. Phys.* **33** (1961) 1.

[6] W.H. Furry, *Note on the Quantum-Mechanical theory of measurement*, *Phys. Rev.*, **49** (1936) 393

[7] R.A. Bertlmann, W. Grimus and B.C. Hiesmayr, *Quantum mechanics, Furry's hypothesis and a measure of decoherence in the $K^0\bar{K}^0$ system*, *Phys. Rev.* **D 60** (1999) 114032

[8] V. Gorini, A. Kossakowski and E.C.G. Sudarshan, J. Math. Phys. *Completely Positive Dynamical Semigroups of N-Level Systems.*, **17** (1976) 821

[9] G. Lindblad, *On the generators of quantum dynamical semigroups*, *Commun. Math. Phys.* **48** (1976) 119

[10] J.R. Ellis, J.S. Hagelin, D.V. Nanopoulos and M. Srednicki, *Search for Violations of Quantum Mechanics*, *Nucl. Phys.* **B 241** (1984) 381

[11] P. Huet and M.E. Peskin, *Violation of CPT and quantum mechanics in the $K^0 - \bar{K}^0$ system*, *Nucl. Phys.* **B 434** (1995) 3 [hep-ph/9403257]

[12] F. Benatti and R. Floreanini, *Completely positive dynamical maps and the neutral kaon system*, *Nucl. Phys.* **B 488** (1997) 335

[13] J. Bernabeu, N.E. Mavromatos and J. Papavassiliou, *Novel type of CPT violation for correlated EPR states, Phys. Rev. Lett.* **92** (2004) 131601 [hep-ph/0310180]

[14] *Handbook on neutral kaon interferometry at a* Φ*-factory*, Ed. A. Di Domenico, *Frascati Physcs Series*, pp. 39-102 and 155-182, Frascati Physics Series vol. XLIII, 2007, ISBN 978-88-86409-50-8

[15] A. Gallo et al., *DAΦNE status report, Conf. Proc.* **C 060626** (2006) 604

[16] M. Adinolfi et al., *The tracking detector of the KLOE experiment, Nucl. Instrum. Meth.* **A 488** (2002) 51

[17] M. Adinolfi et al., *The KLOE electromagnetic calorimeter, Nucl. Instrum. Meth.* **A 482** (2002) 364

[18] M. Adinolfi et al., *The trigger system of the KLOE experiment, Nucl. Instrum. Meth.* **A 492** (2002) 134

[19] F. Ambrosino et al., *Data handling, reconstruction, and simulation for the KLOE experiment, Nucl. Instrum. Meth.* **A 534** (2004) 403 [physics/0404100]

[20] CPLEAR collaboration, A. Apostolakis et al., *An EPR experiment testing the nonseparability of the $K^0\bar{K}^0$ wave function, Phys. Lett.* **B 422** (1998) 339

[21] CPLEAR collaboration, A. Apostolakis et al. *Tests of CPT symmetry and quantum mechanics with experimental data from CPLEAR, Phys. Lett.* **B 364** (1995) 239 [hep-ex/9511001]